Boundary Indicator for Aspect Limited Sensing of Hidden Dielectric Objects

A Boundary Indicator for Aspect Limited Sensing of Hidden Dielectric Objects

Martina T. Bevacqua and Tommaso Isernia, *Senior Member, IEEE*

***Abstract*—This letter addresses the problem of reconstructing the geometrical features, i.e. location, shape and size of targets embedded into a non-accessible region. In particular, an approach recently introduced for the case of free space and full aspect measurements, is extended, discussed and validated for the more realistic and challenging case of data collected under 'aspect limited' measurement configurations, which include subsurface sensing, cross-borehole imaging and many other cases. Results obtained by considering 2D scenario and noise affected simulated data confirm the potentialities of the proposed method in dealing with realistic applications.**

***Index Terms*—Equivalence Theorem, Hidden Objects, Inverse source problem, Microwave Imaging, Shape reconstruction, Sparsity promotion, Subsurface sensing.**

I. Introduction

THE problem of reconstructing the unknown support of an object embedded in a non-accessible region from the measurements of the field which it scatters is relevant in many engineering and science applications [1-3]. With respect to inverse *medium* problems, which aim at recovering both electromagnetic and geometrical properties, in such a problem, known as inverse *obstacle* problem, one can reduce somehow the efforts to determine the solution of the problem [4,5], but by paying the price of dropping the possibility of retrieving the electromagnetic properties of the scatterer.

However, both problems require coping with the solution of a non-linear and ill-posed inverse scattering problem. In addition, these difficulties are further worsened when, as in subsurface sensing, it is not possible to probe the targets from all the different directions, thus entailing an unavoidable deterioration of the imaging result.

In such a circumstance, tomographic inversion techniques based on Born (BA) or Kirchhoff (KA) approximations have been commonly exploited to image hidden target [6,7]. On the other side, these linearized methods, which rely on first order scattering approximations, have a very limited range of validity. Another very popular *qualitative* solution method is the linear sampling method (LSM) [8,9] which solves an auxiliary linear inverse problem instead of a non-linear one and is characterized by a straightforward implementation and real-time processing. Other methods are instead based on the solution of inverse *source* problems [10], which consists in retrieving the currents induced inside the unknown object.

Recently, a novel qualitative method, based on equivalence theorem, solution of a constrained inverse source problem and sparsity promotion has been introduced in literature for the case of a free space background and full aspect measurement set up [11]. The main advantage of this latter is the possibility of processing simultaneously different experiments by enforcing some coherence among them, without any a posteriori combination of the results. Moreover, the method does not require the exact knowledge of the incident fields but only some kinds of diversity in terms of incidence angle and/or frequency. As such, it is robust with respect to model error and knowledge on the background medium.

In this letter, the approach in [11] is extended and tested in the much more realistic and challenging case of aspect limited measurements and geophysical prospecting [6,12-21]. In particular, three different application oriented cases dealing with aspect limited data are considered. The first configuration exploits two different sets of antennas acting both as transmitters and as receivers. In the second configuration, a first set of antennas acts as transmitters and a second one another one acts as receivers. This is the case for instance of cross-borehole sensing, which corresponds to measuring just the transmitted fields, and is generally adopted in imaging deep regions. This configuration is typically used to fracture detection and evaluation, archaeology, cavity detection, metal resources surveys, and reservoir characterization and monitoring [15-19]. Finally, the last measurements configuration just uses a single set of antennas. This is of interest in GPR like sub-surface sensing, which is based on reflected field measurements and is used when only surface measurements can be collected [6,12,21].

The letter is organized as follows. In Section II, the basic mathematical formulation of the inverse scattering problem is recalled. In Sections III a review of the approach described in [11] is given, while in Section IV an assessment of

This is the *postprint* version of the following article: M. T. Bevacqua and T. Isernia, "Boundary Indicator for Aspect Limited Sensing of Hidden Dielectric Objects," in *IEEE Geoscience and Remote Sensing Letters*, vol. 15, no. 6, pp. 838-842, June 2018. doi: 10.1109/LGRS.2018.2813087. Article has been published in final form at: https://ieeexplore.ieee.org/document/8347011.

performances with numerical noisy data is provided in case of dielectric hidden targets. Conclusions follow. Throughout the letter, the canonical 2-D scalar problem (TM polarized fields) is considered. The time-harmonic factor $e^{j\omega t}$ is assumed and dropped.

II. Mathematical Formulation of the Problem

Let us denote with z axis as invariance direction and with Σ the compact, possibly not connected, support of an unknown object with relative permittivity $\varepsilon_s(r)$ and electric conductivity $\sigma_s(r)$, embedded in a medium with features $\varepsilon_b(r)$ and $\sigma_b(r)$, being r the coordinate spanning the generic point belonging to the investigation domain. The unknown scatterer is probed by performed different scattering experiments, which can take advantage from different illumination angles or frequency diversity, or a combination of them. The scattered fields, corresponding to each experiment, are measured by means of receiving antennas located at $\boldsymbol{r_m} \in \Gamma$.

The reconstruction of presence, location and shape of the unknown objects consists in the estimation of the support Σ of the contrast function χ, which encodes the electromagnetic properties of the unknown object, starting from the noisy measured scattered field E_s. The equation relating the scattered field E_s to χ, can be expressed as [4]:

$$E_s(\boldsymbol{r_m}, \upsilon) = \int_{\Sigma} G_b(\boldsymbol{r_m}, \boldsymbol{r'}, \upsilon)\, \chi(r', \upsilon) E_t(\boldsymbol{r'}, \upsilon) d\boldsymbol{r'} = \mathcal{A}_e[W] \tag{1}$$

where υ spans the set Υ of the performed scattering experiments, E_t is the total field induced inside the investigation domain and $W = \chi E_t$ are the contrast sources, i.e. the currents induced inside the target. Finally, G_b is the Green's function pertaining to the background medium, while $\mathcal{A}_e$ is a short notation for the integral radiation operator.

Note that G_b depends on the adopted measurement configurations and a priori information about the background medium. For instance, in case of cross-borehole measurement configuration and underground prospecting, G_b is evaluated as the field radiated in the soil by an elementary electric source placed in the same medium. On the contrary, in case of GPR measurements configuration, G_b is evaluated as the field radiated in the air by an elementary electric source placed in the soil. In both cases it can be numerically computed by exploiting the reciprocity theorem.

The problem (1) is nonlinear and ill posed [5]. However, instead of solving (1) in terms of χ, one can look for the induced currents W, whose support exactly coincides with Σ whatever the set Υ of the performed scattering experiments. This represents a relevant circumstance, as the underlying inverse source problem is linear. On the other side, the solution of such a problem is still a very difficult task, as it is severely ill-posed.

III. A Boundary Indicator For Hidden Target

In inverse source problems, the unknowns of the problem are the contrast sources, which are generally different from zero in each point belonging to Σ.

Nevertheless, by virtue of the equivalence theorem [22], the induced sources W can be substituted by electric and magnetic surface currents. These surface currents are 'equivalent' to the volumetric currents W with respect to the radiation of E_s. This equivalence holds true outside a considered surface which contains the original sources. In the following, it is assumed coinciding with the boundary $\partial\Sigma$ of Σ.

Let us denote with W_s and $\boldsymbol{W}_{m,s}$ the electric and magnetic equivalent currents, respectively. So, for each scattering experiment υ, the problem (1) can be recast as:

$$E_s(\boldsymbol{r_m}, \upsilon) = \mathcal{A}_e{}^{EE}[W_s(\boldsymbol{r}, \upsilon)] + \boldsymbol{\mathcal{A}}_e{}^{EH}\left[\boldsymbol{W}_{m,s}(\boldsymbol{r}, \upsilon)\right] \tag{2}$$

where $\mathcal{A}_e{}^{EE}$ and $\boldsymbol{\mathcal{A}}_e{}^{EH}$ are a short notation of the integral external operators which relate the electric fields to the electric and magnetic surface currents, respectively. Both $\mathcal{A}_e{}^{EE}$ and $\boldsymbol{\mathcal{A}}_e{}^{EH}$ take into account the adopted measurement configurations and priori knowledge on the background medium. In particular, in the case of underground prospecting, $\boldsymbol{\mathcal{A}}_e{}^{EH}$ is evaluated by taking into account the field radiated in the soil/air (in dependence on where the measurements are collected) by an elementary magnetic source placed in the soil.

The problem (2) is again severely ill posed, but advantages can be taken from the fact that the equivalent sources are only distributed over the boundary $\partial\Sigma$ and are sparse in the pixel basis representation. As a consequence, a possible strategy to regularize equation (2) consists in looking for the sparsest current distribution consistent with the measured data [23]. Unfortunately, because of the limited number of independent data that one can collect in each single experiment, the request for sparseness is not sufficient to regularize each single inverse source problems.

In order to overcome such a difficulty, an additional variable $\mathcal{B}$ (see also equation (3) below), defined as the upper bound to the amplitudes of the equivalent currents corresponding to the different scattering experiments, is introduced and considered as an auxiliary unknown of the problem. The introduction of this variable allows to enforce a congruity among the currents corresponding to each scattering experiment belonging to Υ. In fact, whatever υ, the equivalent currents are always localized on its boundary $\partial\Sigma$.

Accordingly, equation (2) can be conveniently solved by enforcing sparsity of $\mathcal{B}$, i.e.:

$$\begin{aligned} &\min \|\mathcal{B}(\boldsymbol{r})\|_1 \\ s.t. \quad &\left\|E_s - \mathcal{A}_e{}^{EE}[W_s] - \boldsymbol{\mathcal{A}}_e{}^{EH}\left[\boldsymbol{W}_{m,s}\right]\right\|_2 \le \delta \\ &|W_s(\boldsymbol{r}, \upsilon)| \le \mathcal{B}(\boldsymbol{r}), \qquad \forall\, \upsilon \in \Upsilon \\ &\frac{\left|\boldsymbol{W}_{m,s}(\boldsymbol{r}, \upsilon)\right|}{\zeta} \le \mathcal{B}(\boldsymbol{r}), \quad \forall\, \upsilon \in \Upsilon \end{aligned} \tag{3}$$

where $\zeta = \sqrt{\mu_b \varepsilon_b{}^{-1}}$ is considered in order to take into account the different units of magnetic and electric currents.

As discussed in [11], solution of problem (3) will be the result of a trade trade-off between sparsity promotion and an

accurate fitting on the data. In fact, the data consistency, enforced by the first constraint, induces solutions with support not smaller than the actual one. On the other hand, the minimization of the l_1 norm of $\mathcal{B}$ entails an estimated support which does not exceed the convex hull of the actual support of the target. For more details about the approach and how to select the δ parameter, the readers are deferred to [11].

IV. Numerical Assessment

To give a proof of the viability of the approach, as well as to understand the kind of performances which can be achieved, some numerical examples dealing with objects hidden in different scenarios are considered in the following.

The scattered field data have been simulated by means of a 2D full wave finite element solver and corrupted by means of white Gaussian noise at a given SNR. For more details about the building of the data matrix, the readers are referred to [12]. Finally, to show the performance achievable by the method, the results have been compared with those obtained with the LSM [9].

As a first example, a through-the-wall imaging scenario with a stratified structure made of five layers is considered, which simulate the walls ($\varepsilon_b = 4$ and $\sigma_s = 0.01$ mS/m) and the interior of a room ($\varepsilon_b = 1$ and $\sigma_s = 0$ mS/m) (see Fig. 1(a)). The dielectric obstacle consists of an ellipse with axis 0.2 m and 0.3 centred at (0.1, 0.1) m in the middle layer (that is the interior of the room) and electromagnetic properties $\varepsilon_b = 2$ and $\sigma_s = 0$ mS/m). The room of 2x2 m2 is probed by two linear arrays 3m long located at two opposite sides of the room, at a distance from the wall equal to 0.3 m. In such a configuration, each antenna acts both as a transmitter and as a receiver, each array is constituted by 5 antennas, and working frequency is 500 MHz. The total number of collected data T, given by the number of scattering experiments (i.e., the number of transmitting antennas) times the number of collected measurement for each experiment, is equal to T=10x10. Note such a number is lower that the number of degrees of freedom of scattered fields [24]. The data have been corrupted with a SNR equal to 30 dB.

The obtained indicators for both the LSM and the proposed approach are reported in figure 1. The results confirm the effectiveness of the proposed strategy in retrieving qualitative information on the anomaly embedded in the inner layer, although both a limited number of incident illuminations and measurements have been considered. Moreover, the effectiveness is also confirmed in case of reduced number of data and a higher amount of noise (SNR=10dB).

In order to test the approach in a harsher scenario, in the second example only transmitted field measurements have been performed. In particular, a cross-borehole measurement configuration is considered where the two boreholes (30 m long) are positioned at 31 m each from the other, hosting 11 evenly spaced probes. To build the data matrix, the reciprocity property has been exploited and a total number of data T=22×22 has been considered. Moreover, its top side is 12 m below the air-soil interface. The scenario consists of a dry soil ($\varepsilon_b = 6$, $\sigma_s = 1$ mS/m), hosting a void mimicking an extended crack ($\varepsilon_b = 1$, $\sigma_s = 0$ mS/m). The working frequency is 18 MHz, while SNR is equal to 30 dB. The investigated domain is a 30×30 m2 square region discretized into 40×40 cells.

The results are shown in figure 2. Again, the LSM works fine if T=22x22 (fig. 2(a)). Then, the reduction of number of both measurements and transmitting antennas negatively affects the LSM map, which progressively becomes unreliable (fig. 2(c)-(d)). On the contrary, the boundary indicator is able to guarantee accurate results also with a number of data T as low as 11x6 (fig. 2(g)). Moreover, the crack is correctly identified also in case of higher amount of noise on data (SNR=10 dB). It is also worth to note that the approach is robust with respect to model error. In fact, data have been simulated by taking into account the presence of the air-soil interface, while in the inversion we have neglected the presence of the interface adopting the homogeneous background Green's function in solving (3) (see figure 2(h)). Also note that thanks to the fact the method just requires diversity amongst the different experiments (and precise knowledge of the incident fields is not required) no information about the actual distance amongst the boreholes has been used in the inversion, which is a further asset towards robust applicability.

In the last example, the surveyed area consists in a soil with $\varepsilon_b = 4$ and $\sigma_s = 1$ mS/m, hosting a plastic mine ($\varepsilon_s = 2.5$, $\sigma_s = 0$ mS/m) and a stone ($\varepsilon_s = 6$, $\sigma_s = 1$ mS/m). The working frequency is 400 MHz, while SNR is equal to 30 dB. The investigated domain is a 1.5×1 m2 region discretized into 50×34 cells. A GPR measurement configuration is considered. The antenna array is 3 m long and is positioned at the air-soil interface, hosting 16 evenly spaced probes.

The obtained LSM indicators corresponding to different number of data and SNR are reported in figures 3(a)-(d), while the normalized boundary indicators $\mathcal{B}$ are shown in figures 3(e)-(h). As it can be seen, the LSM method does not work properly with a reduced number of data. In fact, artifacts appear in as false targets or 'ghosts' in the tomographic images (see figures 3(b)-(d)). It is important to underline that, with respect to the two previous examples, the scenario here considered is more challenging as only reflected field measurements are collected. Moreover, the measurements are just performed on the air-soil interface and the investigated area is only illuminated from the top. Despite these difficulties, the proposed approach is able at least to detect the targets and identify their positions also in case of a reduced number of data T=8×16 and T=8×8 and a SNR equal to 10dB.

V. Conclusion

In this letter, a recent shape reconstruction method is extended and checked for the realistic and challenging case of aspect limited data. The approach, previously introduced for the case of free space and full aspect measurements, is based on the reconstruction of boundary of unknown targets by means of the joint solution of different properly regularized inverse source problems.

The results obtained in three different scenarios, i.e., subsurface sensing, through the wall imaging, and fracture detection, and by considering three different measurement

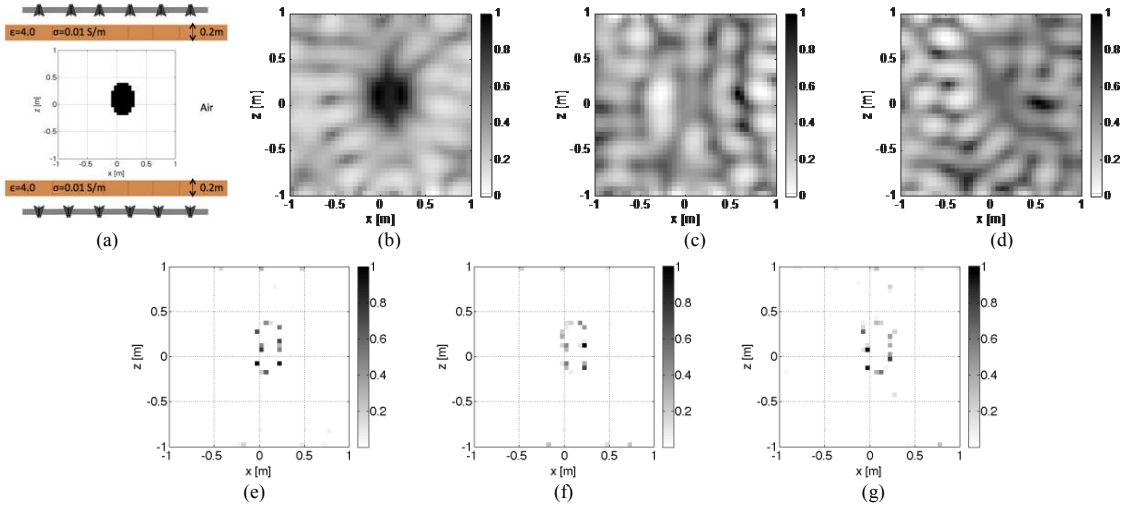

Fig. 1. Dielectric object hosted in a stratified scenario. (a) Sketch of the room. Normalized LSM support indicator corresponding to (b) T=10x10, (c) T=6x10 and (d) T=6x10 with SNR=10dB. Normalized boundary indicator corresponding to (e) T=10x10, (f) T=10x6 and (g) T=10x6 with SNR=10dB ($\delta = 0.3\|E_s\|_2$).

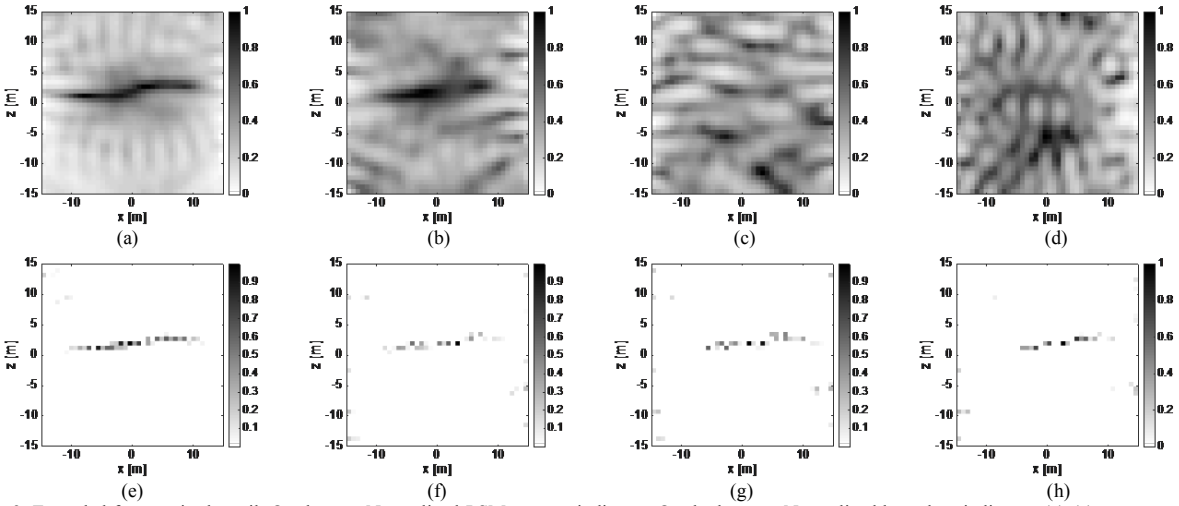

Fig. 2. Extended fracture in the soil. On the top: Normalized LSM support indicator. On the bottom: Normalized boundary indicator. (a)-(e) correspond to a number of data equal to T=22x22, (b)-(f) to T=11x11 and (c)-(g) to T=6x11 ($\delta = 0.3\|E_s\|_2$). (d)-(h) correspond to T=6x11, the presence of model error and SNR=10 dB ($\delta = 0.5\|E_s\|_2$).

configurations, have been compared to the ones obtained with the LSM. Unlike the LSM, the approach guarantees accurate reconstructions of the support of the scatterers or at least their detection. Interestingly, they show adequate performances also when the number of available data is drastically reduced or some kind of uncertainties on the electromagnetic model is taken into account.

REFERENCES

[1] Scapaticci, R., L. Di Donato, I. Catapano, and L. Crocco, "A feasibility study on microwave imaging for brain stroke monitoring," *Progress In Electromagnetics Research B*, Vol. 40, 305-324, 2012.

[2] Bozza, G., M. Brignone, M. Pastorino, M. Piana, and A. Randazzo, "A linear sampling approach to crack detection in microwave imaging," 2008 IEEE International Workshop on Imaging Systems and Techniques, 222-226, Crete, 2008.

[3] I. Akduman, L. Crocco, and F. Soldovieri, "Experimental validation of a simple system for through-the-wall inverse scattering," *IEEE Geosci. Remote Sens. Lett.*, vol. 8, no. 2, pp. 258–262, Mar. 2011

[4] D. Colton and R. Kress. "Inverse Acoustic and Electromagnetic Scattering Theory", *Springer-Verlag,* Berlin, Germany, 1998.

[5] M. Bertero and P. Boccacci, Introduction to Inverse Problems in Imaging, *Institute of Physics*, Bristol, UK, 1998.

[6] R. Persico. Introduction to Ground Penetrating Radar: Inverse Scattering and Data Processing, Wiley, 2014.

[7] F. Soldovieri and L. Crocco. "Electromagnetic Tomography". In: Subsurface Sensing. Ed. by A. S.Turk, K. A. Hocaoglu, and A. A. Vertiy. New York: Wiley, 2011. Chap. 5, pp. 228–254.

[8] Colton, D. and A. Kirsch, "A simple method for solving inverse scattering problems in the resonant region," *Inverse Probl.*, Vol. 12, 383-393, 1996.

[9] Catapano, I., Crocco, L., & Isernia, T., "Improved sampling methods for shape reconstruction of 3-D buried targets". *IEEE Trans. Geosci. Remote Sens.*, *46*(10), 3265-3273, 2008.

[10] S. Sun, B. J. Kooij and A. G. Yarovoy, "Linearized 3-D Electromagnetic Contrast Source Inversion and Its Applications to Half-Space Configurations," in *IEEE Trans. on Geosci. Remote Sens.*, vol. 55, no. 6, pp. 3475-3487, June 2017.

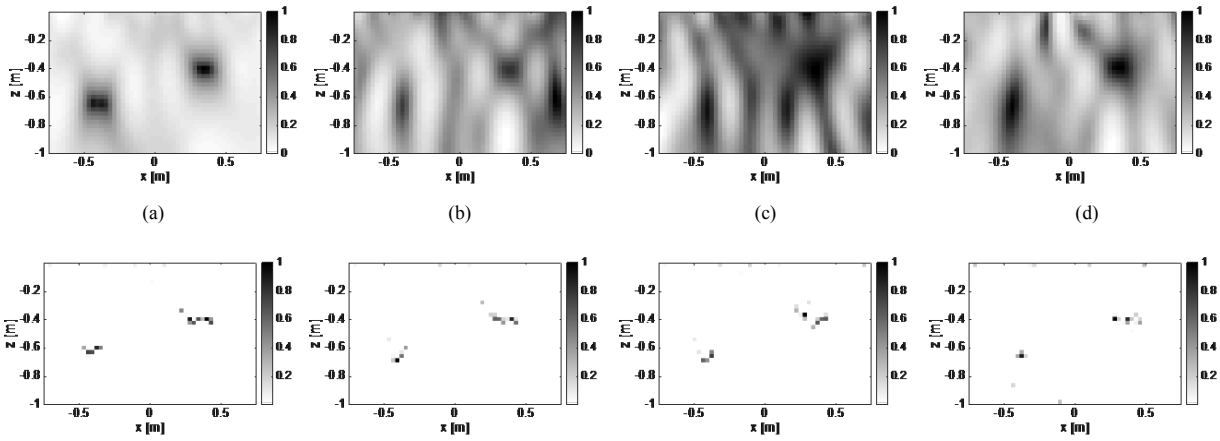

(a) (b) (c) (d)

(e) (f) (g) (h)

Fig. 3. Two dielectric targets buried in the soil. On the top: Normalized LSM support indicator. On the bottom: Normalized boundary indicator. (a)-(e) correspond to a number of data equal to T=16x16 ($\delta = 0.3\|E_s\|_2$), (b)-(f) to T=8x16 ($\delta = 0.3\|E_s\|_2$), (c)-(g) to T=8x16 and SNR=10 dB ($\delta = 0.4\|E_s\|_2$), (d)-(h) to t= 8x8 ($\delta = 0.3\|E_s\|_2$).

[11] M. Bevacqua and T. Isernia, "Shape reconstruction via equivalence principles, constrained inverse source problems and sparsity promotion," *Progress In Electromagnetics Research*, vol. 158, pp. 37–48, 2017.

[12] M. Bevacqua, L. Crocco, L. Di Donato, T. Isernia, R. Palmeri, "Exploiting Field Conditioning and Sparsity for Microwave Imaging of Non-weak Buried Targets", *Radioscience*, 2016. (DOI: 10.1002/2015RS005904).

[13] A. Hoorfar, O. Kilic, and A. E. Fathy, "Compressive Sensing–Based High-Resolution Imaging and Tracking of Targets and Human Vital Sign Detection behind Walls", In: C.H. Chen, Compressive Sensing of Earth Observations, chapter no.3, published by CRC Press [Book # K29608].

[14] L. Song, C. Yu and Q. H. Liu, "Through-wall imaging (TWI) by radar: 2-D tomographic results and analyses," in *IEEE Trans on Geosci. Remote Sens*, vol. 43, no. 12, pp. 2793-2798, Dec. 2005.

[15] H. Zhou and M. Sato, "Fracture imaging and saline tracer detection by crosshole borehole radar data migration," in Proc. 8th Int. Conf. Ground Penetrating Radar, vol. 4084, SPIE, D. A. Noon, G. F. Stickley, and D. Longstaff, Eds., 2000, pp. 303–307.

[16] H. Zhou and M. Sato, "Application of vertical radar profiling technique to Sendai Castle," *Geophysics*, vol. 65, pp. 533–539, Mar.-Apr. 2000.

[17] H. Choi and J. Ra, "Detection and identification of a tunnel by iterative inversion from cross-borehole CW measurements," *Microwave Opt.Technol. Lett.*, vol. 21, pp. 458–465, June 1999.

[18] P. K. Fullagar et al., "Radio tomography and borehole radar delineation of the McConnell nickel sulfide deposit, Sudbury, Ontario, Canada," Geophysics, vol. 65, pp. 1920–1930, Nov.-Dec. 2000.

[19] M. Li, A. Abubakar, T.H. Habashy, "Application of a two-and-a-half dimensional model-based algorithm to crosswell electromagnetic data inversion", *Inverse Problems*, vol. 26, n. 7, 2010.

[20] O. Semerci, G. Pan, M. Li, L. Liang, T.H. Habashy, "Joint electromagnetic and seismic inversion for petrophysical parameters using multi-objective optimization", *in SEG Technical Program Expanded Abstracts 2014, Society of Exploration Geophysicists*, pp. 733-738, 2014.

[21] D. J. Daniels. Ground Penetrating Radar, 2-nd edition. London, UK: The Institution of Electrical Engineers, 2004.

[22] Franceschetti, G., Electromagnetics: Theory, Techniques, and Engineering Paradigms, Springer Science & Business Media, 2013.

[23] Donoho, D., "Compressed sensing," *IEEE Trans. Inf. Theory*, Vol. 52, No. 4, 1289-1306, 2006.

[24] O. M. Bucci and Isernia T., "Electromagnetic inverse scattering: Retrievable nformation and measurement strategies", *Radio Sci*., 32: 2123–2138, 1997.